

# $^1\text{H}$ Dynamic NMR and X-ray crystal structure studies of conformational preferences in dibenzo[*c,h*][1,6]diazecines

Silke Lehmann,<sup>a,\*</sup>† Gerald W. Buchanan,<sup>a</sup> Corinne Bensimon,<sup>b</sup>  
Jens Hartmann<sup>c</sup> and Werner Schroth<sup>c,\*</sup>

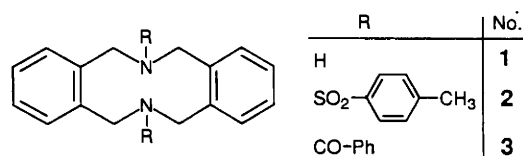
<sup>a</sup> Dept. of Chemistry, Carleton University, Ottawa, Ontario, K1S 5B6, Canada

<sup>b</sup> Dept. of Chemistry, University of Ottawa, Ottawa, Ontario, K1N 6N5, Canada

<sup>c</sup> Institut für Organische Chemie, FB Chemie, Martin-Luther-Universität, Halle-Wittenberg, PF 8, 06099 Halle/S., Germany

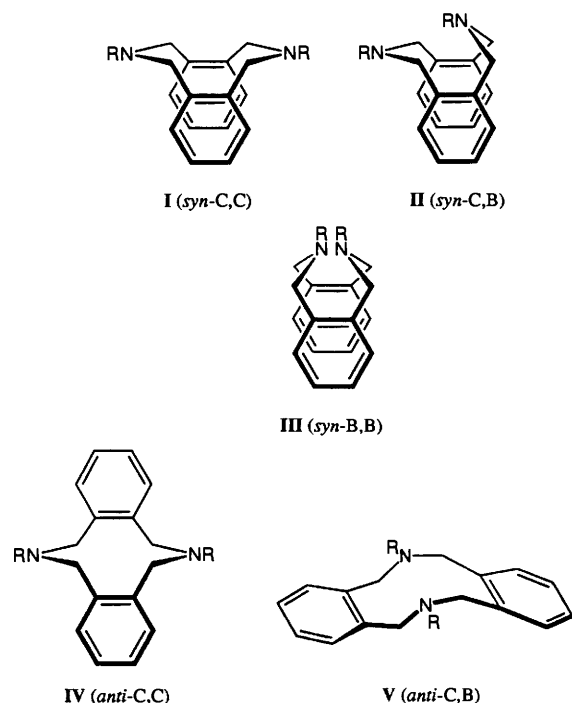
The conformational equilibria and preferences in dibenzo[*c,h*][1,6]diazecines have been investigated by  $^1\text{H}$  DNMR measurements and X-ray crystallography. It has been found that restricted rotation about the exocyclic N–S bond in 6,13-ditosyl-6,7,13,14-tetrahydro-5*H*,12*H*-dibenzo[*c,h*][1,6]diazecine **2** becomes slow on the NMR timescale in the temperature range 200–300 K. The free energy of activation was determined to be  $43.5 \pm 0.5 \text{ kJ mol}^{-1}$  for this dynamic process. Steric hindrance at the transition state is deemed to be the most important contribution to the N,S barrier. From X-ray crystal structure analyses, it appears that the influence of the N-inversion on this barrier is negligible. The conformation in the solid state is also the preferred one in solution. The X-ray structure illustrates the spatial vicinity of the tosyl groups relative to the annelated benzene moieties of the 10-membered ring. Consistent with these results are high field shifts and corresponding splittings in the aromatic part of the  $^1\text{H}$  NMR spectrum of compound **2**.

Hydrogenolytic cleavage of the N–N bond in 5*H*,7*H*,12*H*,14*H*-phthalazino[2,3-*b*]phthalazine with Raney nickel in ethanol gave directly 6,7,13,14-tetrahydro-5*H*,12*H*-dibenzo[*c,h*][1,6]diazecine **1**, which was tosylated to give the derivative **2**.<sup>1</sup> Recently conformational analysis was carried out for the dibenzo[*c,h*][1,6]diazecines **1**–**3** by means of  $^1\text{H}$  and  $^{13}\text{C}$  DNMR spectroscopy.<sup>2</sup>



Owing to rigid structural units in the 10-membered rings of **1**–**3** only five preferred conformers, I–V, should be possible. All others are destabilized by steric interactions.<sup>2,3</sup> In contrast to **2** the compounds **1** and **3** were found to be chair conformers IV. For compound **2** a *syn* conformation was proposed.<sup>2</sup> The different conformational behaviour of **2** vs. **1** and **3** could not be explained previously and is the subject of our present study.

The  $^1\text{H}$  DNMR measurements were repeated in  $\text{CD}_2\text{Cl}_2$ . At room temperature all dynamic processes are fast in the NMR timescale and a sharp singlet was observed for the  $\text{CH}_2$  protons of compound **2**. On lowering the sample temperature not only did the signal for the  $\text{CH}_2$  protons split up, but those of the aromatic protons did too. Questions arise as to which kind of dynamic process occurs: (i) restricted rotation about the exocyclic N–S bond, (ii) N-inversion or (iii) a 10-membered ring inversion process. In addition, one would like to know the nature of the ground-state conformations of these molecules. In



order to determine these, the X-ray crystal structures have now been obtained for **1** and **2**.

## Experimental

### $^1\text{H}$ DNMR Measurements

The NMR spectra were recorded at 400.13 MHz on a Bruker AMX 400 spectrometer with a computer-controlled temperature unit (accuracy  $\pm 1 \text{ K}$ ). In order to determine the dynamic parameters, the spectra were recorded every  $5^\circ$ . Chemical shifts ( $\delta$ ) are given with reference to TMS.

† Present address: Institut für Analytik und Umweltchemie, FB Chemie, Martin-Luther-Universität Halle-Wittenberg, PF 8, 06099 Halle/S., Germany.

**Table 1** Crystal data and experimental details

	1	2
Formula	C <sub>16</sub> H <sub>18</sub> N <sub>2</sub>	C <sub>30</sub> H <sub>30</sub> N <sub>2</sub> S <sub>2</sub> O <sub>4</sub>
Formula weight	238.33	546.70
Crystal shape	Plate	Cube
Crystal size/mm	0.2, 0.2, 0.05	0.2, 0.2, 0.2
Crystal system	Monoclinic	Monoclinic
<i>a</i> /Å	10.0243(24)	14.526(4)
<i>b</i> /Å	4.9608(8)	6.3906(18)
<i>c</i> /Å	13.158(4)	14.868(4)
$\beta$ /°	107.076(22)	107.123(21)
<i>V</i> /Å <sup>3</sup>	625.5(3)	1319.1(6)
Space group	<i>P</i> 2 <sub>1</sub> / <i>c</i>	<i>P</i> 2 <sub>1</sub> / <i>a</i>
<i>Z</i>	2	4
<i>D<sub>x</sub></i> /g cm <sup>-3</sup>	1.265	1.376
<i>F</i> (000)	256.08	575.92
$\mu$ /mm <sup>-1</sup>	0.14	0.23
$\lambda$ /Å	0.7093	0.7093
<i>h, k, l</i> ranges	-11 ≤ <i>h</i> ≤ 11, 0 ≤ <i>k</i> ≤ 5, 0 ≤ <i>l</i> ≤ 15	-15 ≤ <i>h</i> ≤ 15, 0 ≤ <i>k</i> ≤ 7, 0 ≤ <i>l</i> ≤ 17
<i>R<sub>f</sub></i> (sign refl)	0.063	0.040
<i>R<sub>w</sub></i> (sign refl)	0.038	0.028
<i>R<sub>f</sub></i> (all refl)	0.084	0.053
<i>R<sub>w</sub></i> (all refl)	0.038	0.028
Goodness of fit	5.49	3.33

### Crystal data and X-ray structure analysis

All measurements were made on a Rigaku diffractometer with Mo-K $\alpha$  radiation. In each case the crystals were mounted on glass capillaries. Cell constants and orientation matrices for data collection were obtained from least-squares refinement using the setting angles of 25 reflections in the range  $40 < 2\theta < 50^\circ$ , corresponding to monoclinic cells. The data were collected at a temperature of  $-110^\circ\text{C}$  using the  $\omega$ - $2\theta$  scan technique to a maximum  $2\theta$  value of  $49.9^\circ$ . Experimental details and crystal data are summarized in Table 1. For compound **1** a total of 1158 reflections were collected; the unique set contains 1094 reflections. In the case of compound **2** a total of 2357 reflections were collected; the unique set contains 2253 reflections. The standards were measured after every 150 reflections. No crystal decay was noticed. The data were corrected for Lorentz and polarisation effects.<sup>4</sup> No absorption correction was made. The structures were solved by direct methods. All the atoms except the hydrogen were refined anisotropically. The hydrogen atoms were found from a difference Fourier map. The final cycle of full matrix least-squares refinement was based on 838 observed reflections [ $I > 2.5\sigma(I)$ ] and 119 variable parameters for compound **1**. For **2** it was based on 1828 observed reflections [ $I > 2.5\sigma(I)$ ] and 233 variable parameters. Weights based on counting statistics were used. The maximum and minimum peaks on the final difference Fourier map corresponded to 0.350 and  $-0.280 e/a^3$ , respectively (compound **1**), and to 0.340 and  $-0.350 e/a^3$ , respectively (compound **2**).

All calculations were performed using the NRCVAX crystallographic software packages.<sup>5</sup> Atomic coordinates, bond lengths and angles, and thermal parameters have been deposited at the Cambridge Crystallographic Data Centre.†

## Results and discussion

### <sup>1</sup>H DNMR

The <sup>1</sup>H and <sup>13</sup>C NMR spectra of compounds **1–3** and the corresponding dynamic NMR parameters in CFC<sub>3</sub> have already been published.<sup>2</sup> Hence NMR data of compounds **1** and **3** are reported here only in so far as they are necessary to explain the dynamics of conformer interchange in compound **2**.

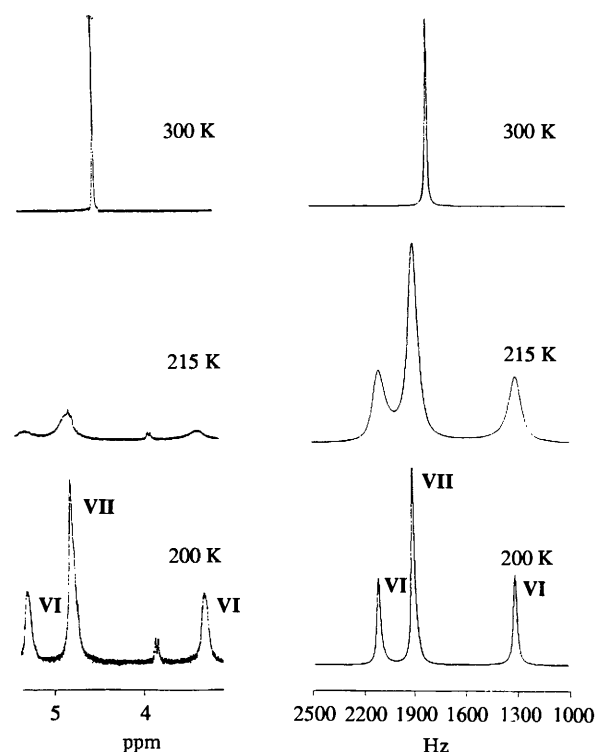


**Fig. 1** Experimental (left) and simulated (right) spectra of the CH<sub>2</sub>-region of compound **2** VI and VII: CH<sub>2</sub>-resonances of the conformers VI and VII, respectively

The <sup>1</sup>H NMR spectra of **2** in CD<sub>2</sub>Cl<sub>2</sub> are temperature-dependent in the range 200–300 K. In fact, a splitting of the CH<sub>2</sub> singlet in four resonances was observed passing through coalescence. Two of them are overlapping as may be seen from the corresponding data in Table 2.

In order to determine the dynamic parameters of this four site case a total line shape analysis was performed with the DNMR5 software.<sup>6</sup> The *T*<sub>2</sub> values were estimated from linewidth changes of the TMS resonance. The CH<sub>2</sub> region of three experimental spectra accompanied by the simulated ones is displayed in Fig. 1.

In contrast to compounds **1**, **3** and other bis(benzo-annulated)(3.3)orthocyclophanes,<sup>2,3</sup> the line shape of the

† For details of the CCDC deposition scheme, see 'Instructions for Authors (1996)', *J. Chem. Soc., Perkin Trans. 2*, 1996, Issue 1.

**Table 2**  $^1\text{H}$  NMR data of compounds **2** and **3** ( $\text{CD}_2\text{Cl}_2$ , TMS)

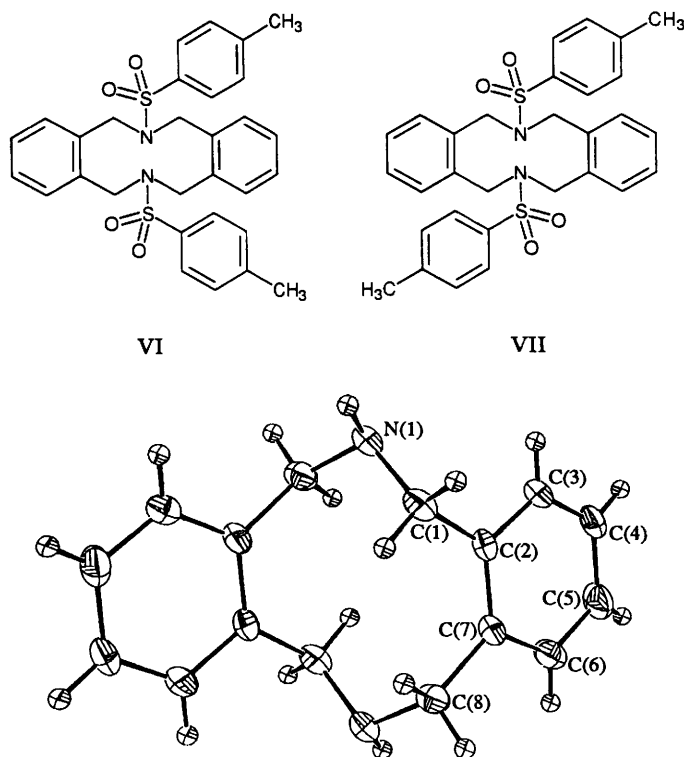
<i>T</i> /K	Compound	Chemical shifts, $\delta$		
		$-\text{CH}_2-$	$=\text{CH}-$	Substituents
300	<b>2</b>	4.48 (s)	6.95–6.97 (m) 6.86–6.89 (m)	7.76 (d); 7.42 (d); 2.48 (s)
	<b>3</b> <sup>a</sup>	4.62 (s, br) 4.28 (s); <sup>b</sup> 4.30 (s) <sup>c</sup>	7.22–7.54 (m)	7.22–7.54 (m)
200	<b>2</b>	4.78 (s, br) 5.29 (s, br); 3.27 (s, br)	7.31 (m); 6.58 (m) 6.95 (m); 6.80 (m)	7.87 (m); 7.73 (m) 7.53 (m) 2.53 (s)
	<b>3</b> <sup>a</sup>	3.64 (d); <sup>b</sup> 3.61 (d) <sup>c</sup> 4.13 (d); <sup>b</sup> 4.08 (d) <sup>c</sup> 4.53 (d); <sup>b</sup> 4.43 (d) <sup>c</sup> 5.48 (d); <sup>b</sup> 5.56 (d) <sup>c</sup>	7.12–7.58 (m)	7.12–7.58 (m)

<sup>a</sup> See ref. 2. <sup>b</sup> Minor isomer. <sup>c</sup> Major isomer.

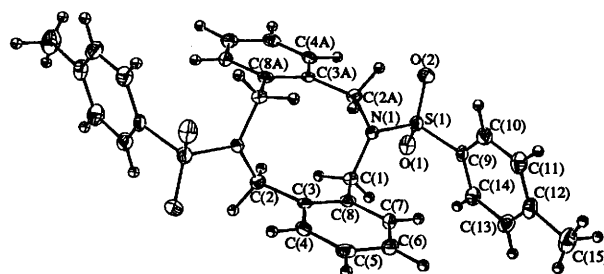
**Table 3** Dynamic parameters of the restricted rotation about the exocyclic N–S bond in compound **2** ( $\text{CD}_2\text{Cl}_2$ ; signal studied:  $-\text{CH}_2-$ )

<i>T</i> /K	<i>P</i> 1 <sup>a</sup>	<i>P</i> 2 <sup>b</sup>	<i>T</i> <sub>2</sub> /s	<i>k</i> /s <sup>-1</sup>	$\Delta G^\ddagger$ /kJ mol <sup>-1</sup>
200	0.49	0.51	0.09	18	43.46
215	0.455	0.545	0.1	120	43.46
230	0.465	0.535	0.13	610	43.52
245	0.46	0.54	0.29	2 100	43.97
260	0.47	0.53	0.32	11 000	43.22
275	0.46	0.54	0.35	32 500	43.36
300	0.46	0.54	0.4	185 000	43.19

<sup>a</sup> Population of the conformer **VI**. <sup>b</sup> Population of the conformer **VII**.  
<sup>c</sup> See ref. 7

**Fig. 2** ORTEP drawing and numbering of the atoms in compound **1**

aromatic protons of **2** changes with the temperature. Considering this effect, the dynamic process, which becomes slow in the temperature range 200–300 K, must be the restricted rotation about the N–S bond. The two conformers **VI** and

**Fig. 3** ORTEP drawing and numbering of the atoms in compound **2**

**VII** are involved in the exchange reaction. Their populations are given in Table 3. For the band-shape simulation the conformer populations are assumed to be temperature dependent. They are not obtained in the iterative way.

If only the ring inversion were slow on the NMR timescale, the line shapes of the aromatic protons would remain unchanged<sup>2</sup> and clear doublets for the diastereotopic  $\text{CH}_2$  protons should be found; if both dynamic processes were slowed down, two sets of four diastereotopic  $\text{CH}_2$  protons, like in the case of compound **3** (see Table 2), are to be expected.

The free energy of activation was determined to be  $43.5 \pm 0.5$  kJ mol<sup>-1</sup>. Similar rotational barriers around the N–S bond were found in dialkylsulfamoyl chlorides.<sup>8</sup> The result was explained in terms of a directional dependent  $p_\pi-d_\pi$  bond which is enhanced by the electronegative chlorine substituent on the sulfur atom. On the other hand, the NMR spectra of  $\text{Et}_2\text{NSO}_2\text{Ph}$  in  $\text{CH}_2\text{Cl}_2$  remained unchanged down to  $-90^\circ$ .<sup>8</sup> In the case of compound **2** partial multiple bonding which involves sulfur d orbitals is possible, too. However, steric hindrance at the transition state should be the most important contribution to the sulfonamide torsional barrier.

X-Ray structure analyses were made to gain information about (i) the influence of the N-inversion on the N,S barrier and (ii) the molecular structures in the solid state.

#### Crystal structures

Drawings of the X-ray structures of compounds **1** and **2** are given in Figs. 2 and 3 together with the atom numbering. Selected bond distances, bond angles and torsional angles are presented in Tables 4 and 5. Both compounds show clearly the chair conformation **IV**, but there are remarkable differences in the  $\text{sp}^2$  character of the nitrogens involved in the 10-membered rings.

The bond distances for both N1–C1 and N1–C8A are 1.479(4) Å and the bond angle C1–N1–C8A is  $114.47(23)^\circ$  in compound **1**. For compound **2** the bond distance N1–C1 is 1.471(4) Å, the

**Table 4** Selected bond distances (Å) and bond angles (°) for compound **1**; esds in parentheses

N1-C1	1.479(4)	C7-C8	1.536(4)
N1-C8A	1.479(4)	C8-N1A	1.479(4)
C1-C2	1.513(5)		
C1-N1-C8A	114.47(23)	C2-C7-C8	123.0(3)
N1-C1-C2	112.1(3)	C6-C7-C8	118.4(3)
C1-C2-C3	117.3(3)	N1A-C8-C7	115.2(3)
C1-C2-C7	124.4(3)		

**Table 5** Selected bond distances (Å), bond angles (°) and torsion angles (°) for compound **2**; esds in parentheses

S1-O1	1.4459(21)	N1-C2A	1.479(3)
S1-O2	1.4419(21)	C1-C8	1.526(4)
S1-N1	1.6323(22)	C2A-C3A	1.524(4)
S1-C9	1.770(3)	C3A-C8A	1.406(4)
N1-C1	1.471(4)		
O1-S1-O2	119.84(13)	N1-C1-C8	112.87(23)
O1-S1-N1	107.41(12)	N1-C2A-C3A	110.72(22)
O1-S1-C9	107.30(13)	C2A-C3A-C4A	117.81(23)
O2-S1-N1	107.19(12)	C2A-C3A-C8A	123.45(24)
O2-S1-C9	108.79(13)	C1-C8-C7	118.47(23)
N1-S1-C9	105.43(12)	S1-C9-C10	119.57(22)
S1-N1-C1	119.37(17)	S1-C9-C14	119.39(22)
S1-N1-C2A	121.33(18)	C11-C12-C15	121.1(3)
C1-N1-C2A	118.88(20)	C13-C12-C15	120.2(3)
O1-S1-N1-C1	44.5(1)	S1-C9-C10-C11	172.9(3)
O2-S1-N1-C1	174.5(2)	C15-C12-C13-C14	178.3(3)
C9-S1-N1-C1	-69.7(2)	O1-S1-N1-C2A	-143.0(2)
O1-S1-C9-C10	169.9(2)	O2-S1-N1-C2A	-13.0(1)
O2-S1-C9-C10	38.9(1)	C9-S1-N1-C2A	102.8(2)
N1-S1-C9-C10	-75.8(2)	O1-S1-C9-C10	-16.2(1)
S1-N1-C1-C8	122.3(2)	O2-S1-C9-C14	-147.3(2)
S1-N1-C2A-C3A	110.3(2)	N1-S1-C9-C14	98.0(2)
N1-C1-C8-C7	-78.5(2)	C2A-N1-C1-C8	-50.4(2)
C2-C3-C4-C5	-179.3(3)	C1-N1-C2A-C3A	-77.2(2)
C6-C7-C8-C1	-176.5(3)	N1-C2A-C3A-C4A	-60.2(2)

bond distance N1-C2A is 1.479(3) Å and the bond angle C1-N1-C2A is 118.88(20)°. That means, that only in compound **1** is the N-inversion to be considered, for the nitrogen atoms in **2** the sp<sup>2</sup> character is predominant. In this way the X-ray data of compound **2** confirm that the dynamic process observed in the DNMR study is the restricted rotation about the exocyclic N-S bond.

Compound **3** could not be obtained in crystalline form suitable for X-ray analysis. Corresponding to X-ray data of related compounds<sup>9,10</sup> the torsion angle between the nitrogen

and an *ortho*-carbon of the phenyl ring in the *N*-benzoyl group of **3** should be *ca.* 60°. In compound **2** the torsion angles N1-S1-C9-C10 and N1-S1-C9-C14 are -75.8 and 98.0°, respectively. Compared with **2**, increased van der Waals and torsional interactions between the 10-membered rings and the *N*-substituents should be observed for compound **3**. However, the main reason for the much higher C,N barrier ( $\Delta G_c^\ddagger = 69.2$  kJ mol<sup>-1</sup>)<sup>2</sup> is the well known strong mesomerism of the amide structure.<sup>11</sup>

The conformation in the solid of compound **2** appears to be the preferred one in solution, too. Compared with the reference value in *o*-xylene ( $\delta = 7.15$ ) the aromatic protons of the annelated benzene rings in **2** show shifts to higher field (up to  $\delta$  6.58; see Table 2). The reason therefore is the spatial vicinity of the tosyl groups relative to the annelated benzene moieties of the 10-membered ring (see Fig. 3). The ring current effect of the aromatic rings in the tosyl substituents causes distinct high field shifts for the protons of the annelated benzene moieties. Besides, the <sup>1</sup>H NMR spectrum of these protons is of ABCD-type proving that the stereoisomer **VII** must be present in solution.

### Acknowledgements

S. Lehmann thanks the Deutscher Akademischer Austauschdienst for supporting this work by a grant. The experimental assistance of Mr K. Bourque to record the <sup>1</sup>H DNMR spectra is acknowledged.

### References

- 1 J. Hartmann, Ph.D. Thesis, Martin-Luther-Universität Halle-Wittenberg, 1990.
- 2 E. Kleinpeter, J. Hartmann and W. Schroth, *Magn. Reson. Chem.*, 1990, **28**, 628.
- 3 Y.-H. Lai and M. Nakamura, *J. Org. Chem.*, 1988, **53**, 2360.
- 4 D. F. Grant and E. J. Gabe, *J. Appl. Crystallogr.*, 1978, **11**, 114.
- 5 E. J. Gabe, F. L. Lee and Y. Lepage, *J. Appl. Crystallogr.*, 1989, **22**, 384.
- 6 D. S. Stephenson and G. Binsch, QCPE Program 365, 1979.
- 7 J. Sandström, *Dynamic NMR Spectroscopy*, Academic Press, London, 1982.
- 8 W. B. Jennings and R. Spratt, *J. Chem. Soc. D*, 1970, 1418.
- 9 U. Lepore, P. Ganis, G. Bombieri, G. Gilli and G. Montaudo, *Cryst. Struct. Commun.*, 1977, **6**, 7.
- 10 E. Arte, J. Feneau-Dupont, J. P. Declercq, G. Germain and M. van Meerssche, *Cryst. Struct. Commun.*, 1977, **6**, 767.
- 11 W. E. Stewart and T. H. Sidall, *Chem. Rev.*, 1970, **70**, 517.

Paper 5/01832C

Received 22nd March 1995

Accepted 11th September 1995